

Abstract

People living with HIV (PLWH) face greater risk of secondary illnesses, chronic inflammation, cancer, and other diseases despite undetectable viral load when treated with combined antiretroviral therapy (cART).

Our lab identified a plausible cause for these comorbidities: cART treatment attenuates the expression of IKAROS, a negative regulator of inflammation in monocyte derived macrophages (MDMs) of PLWH. These MDMs exhibited a trained, hyperresponsive phenotype indicated by increased pro-inflammatory signals and oxidative phosphorylation when challenged with Lipopolysaccharide (LPS).

To investigate this relationship further, we sought to determine if THP1 cells- a human leukemia monocytic cell line- and primary MDMs from HIV (-) controls receiving cART shows downregulation of IKAROS and metabolic changes consistent with those from PLWH derived MDMs.

Methods

Primary cells. CD14⁺CD16⁻ cells were isolated by negative selection (STEMCELL Technologies) from 40 ml of whole blood from volunteers (PLWH and HIV⁻ controls). Cells were plated in RPMI 1640 (Gibco) (SFM) supplemented with 1 mM Sodium Pyruvate, 2 mM Glutamax (serum-free medium, SFM) for 1 hour (to allow cell attachment) before the addition of 10% FBS (Hyclone Defined FBS, Gibco) and human recombinant GM-CSF (25 ng/ml, R&D Systems). **THP1 cells** were cultured in RPMI supplemented with 10% FBS, 10mM Sodium Pyruvate, 2mM Glutamax and Pen/Strep.

Cell metabolism assays. Metabolism of THP1 cells and primary HIV (-) control MDMs was evaluated using the Seahorse XFe96 Flux Analyzer (Agilent, Santa Clara, CA). Antiretroviral drugs were tenofovir (TDF) 320ng/mL, emtricitabine (EMT) 1ug/mL, raltegravir (RAL) 1ug/mL, or their combination (cART). THP1 were treated for 2 days and 80,000/well were plated in the 96-well XFe96 cell culture microplate (Agilent). Freshly isolated primary cells were counted, seeded into a in SFM for 1 hour followed by normal growth medium at the concentration of 35,000 cells/well. On the day of the assay, the medium was replaced with the Seahorse medium (RPMI 1640, Agilent) and the plate was incubated for at least 45 minutes at 37 °C without CO₂ before proceeding with the mitochondrial or the glycolytic stress tests. Mitochondrial function was analyzed using the Seahorse XF Cell Mito Stress Test kit (Agilent). This test measures the Oxygen Consumption Rate (OCR) at baseline and after the sequential injections of oligomycin [inhibitor of electron transport chain (ETC) Complex V, 2 μM], FCCP [ETC uncoupling factor, 2 μM for THP1 and 4 μM for primary cells], and rotenone/antimycin A (inhibitor of ETC Complex I/III, 1 μM). The last injection included Hoechst dye for cell counting and normalization (final concentration 4 mM). Extracellular acidification rate (ECAR) was measured at the same time as OCR. Spare respiratory capacity is the difference between maximal respiration and basal respiration. Glycolysis was assessed with the Seahorse XF Glycolysis Stress Test kit (Agilent). The test measures ECAR at baseline and after three consecutive injections of glucose (10 mM), oligomycin (2 μM), and 2-deoxy-D-glucose together with Hoechst dye (2-DG, 50 mM). Glycolytic reserve is the difference between the glycolytic capacity after oligomycin stimulation and glycolysis measured after glucose injection. OCR and ECAR values were normalized by the number of cells. Total number of cells present in the well upon termination of Seahorse assay was determined by extrapolation using a cell-type specific calibration curve previously created with Hoechst staining by plating an increasing number (from 2,500 to 100,000) of primary monocytes into a Seahorse 96-well XFe96 plate. The cell number and cell type -specific fluorescence was measured from the entire surface of the well, minimizing errors related to the uneven cell distribution. The plate was read at 350 nm excitation and 461 nm emission in the Sinegy Neo2 Multi-mode Microplate Reader (BioTek). SEM derives from assays run in quadruplicates or quintuplicates.

Western blots. Cells were washed twice in cold PBS (Gibco) and lysed with modified RIPA buffer (50 mM Tris, pH 7.4, 150 mM NaCl, 1% NP-40, 1 mM EGTA, pH 7.4, 0.25% sodium deoxycholate) supplemented with 1 mM PMSF, 1 mM sodium orthovanadate (NA3VO4), and phosphatase and protease inhibitor cocktails (Sigma). Whole-cell lysates were kept on ice for 20 min and then centrifuged for 30 min at 14,000 rpm at 4 °C in a microcentrifuge to remove genomic DNA and membranes. Next, lysates (25 to 35 μg) were separated on a 4–15% SDS-PAGE gel (Mini-PROTEAN TGX Precast Gel, Bio-Rad) and transferred to a 0.2 μm nitrocellulose (Trans-Blot Turbo Mini 0.2 μm Nitrocellulose Transfer Packs, Bio-Rad, Hercules, CA) using the Trans-Blot TURBO apparatus (Bio-Rad, Hercules, CA). IKAROS and GAPDH antibodies were from Cell Signaling.

Figure 2. Antiretroviral Treatment Modulates Metabolism of MDM obtained from HIV (-) individuals

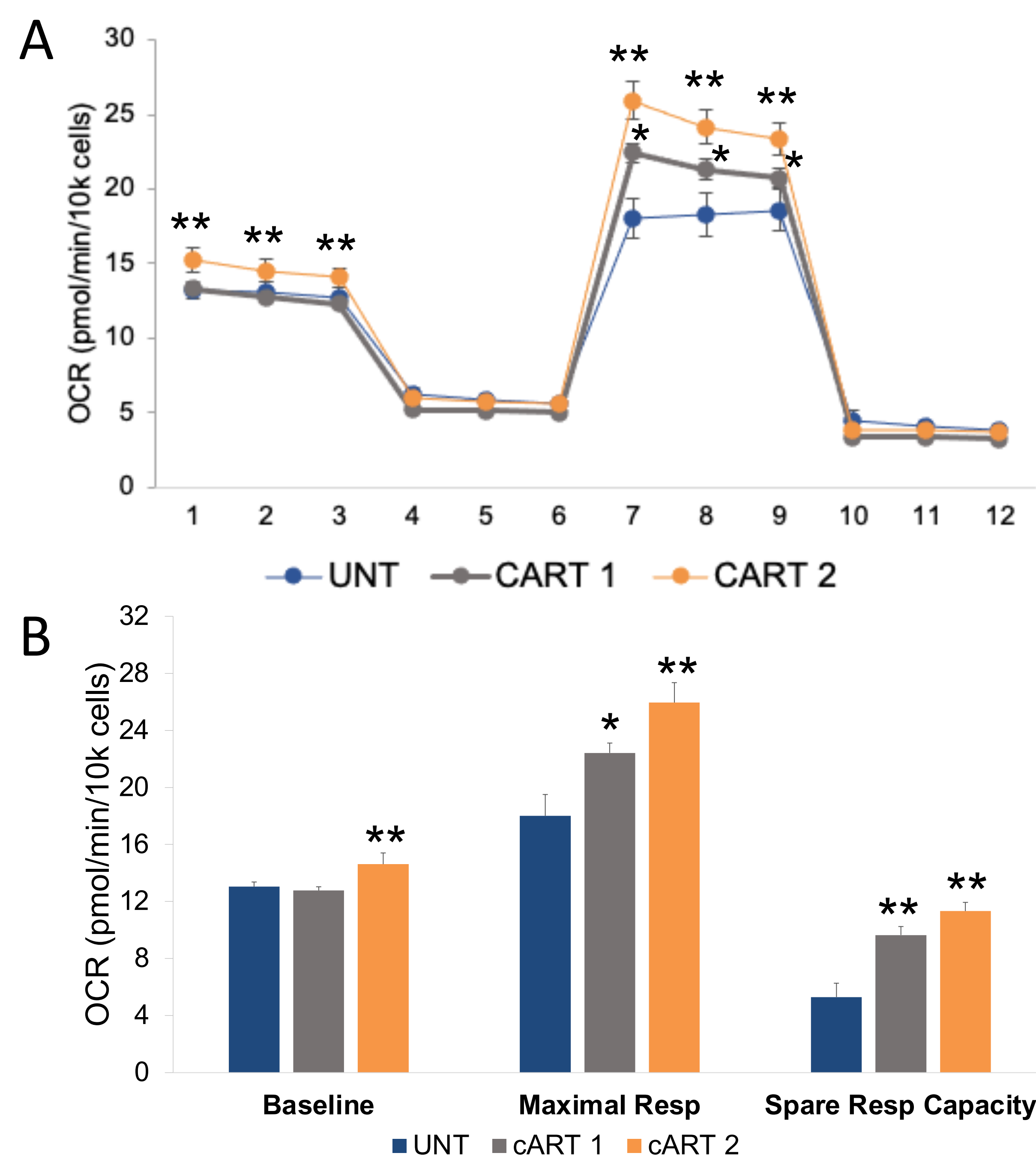


Figure 2. Primary monocytes treated for three days with different concentrations of antiretrovirals, cART1 TDF (320ng/mL), EMT (9.9ng/mL), and RAL (1.8ng/mL). cART2 TDF (320ng/mL), EMT (1μg/mL), RAL (1μg/mL). **A)** Metabolic profile of mitochondrial stress test performed with seahorse bioanalyzer. **B)** Bar graphs representing calculated baseline respiration, maximal respiration, and spare respiratory capacity for mitochondrial stress test. Both cART1 and cART2 increased oxygen consumption at maximal respiration and spare respiratory capacity relative to untreated control MDMs. cART1 increased oxygen consumption in all three measurements and had the greatest absolute increase for each. *indicates p≤0.01, ** P≤0.01 for cART1 or cART2 vs UNT controls

Figure 1. Antiretroviral Treatment Modulates THP1 Metabolism

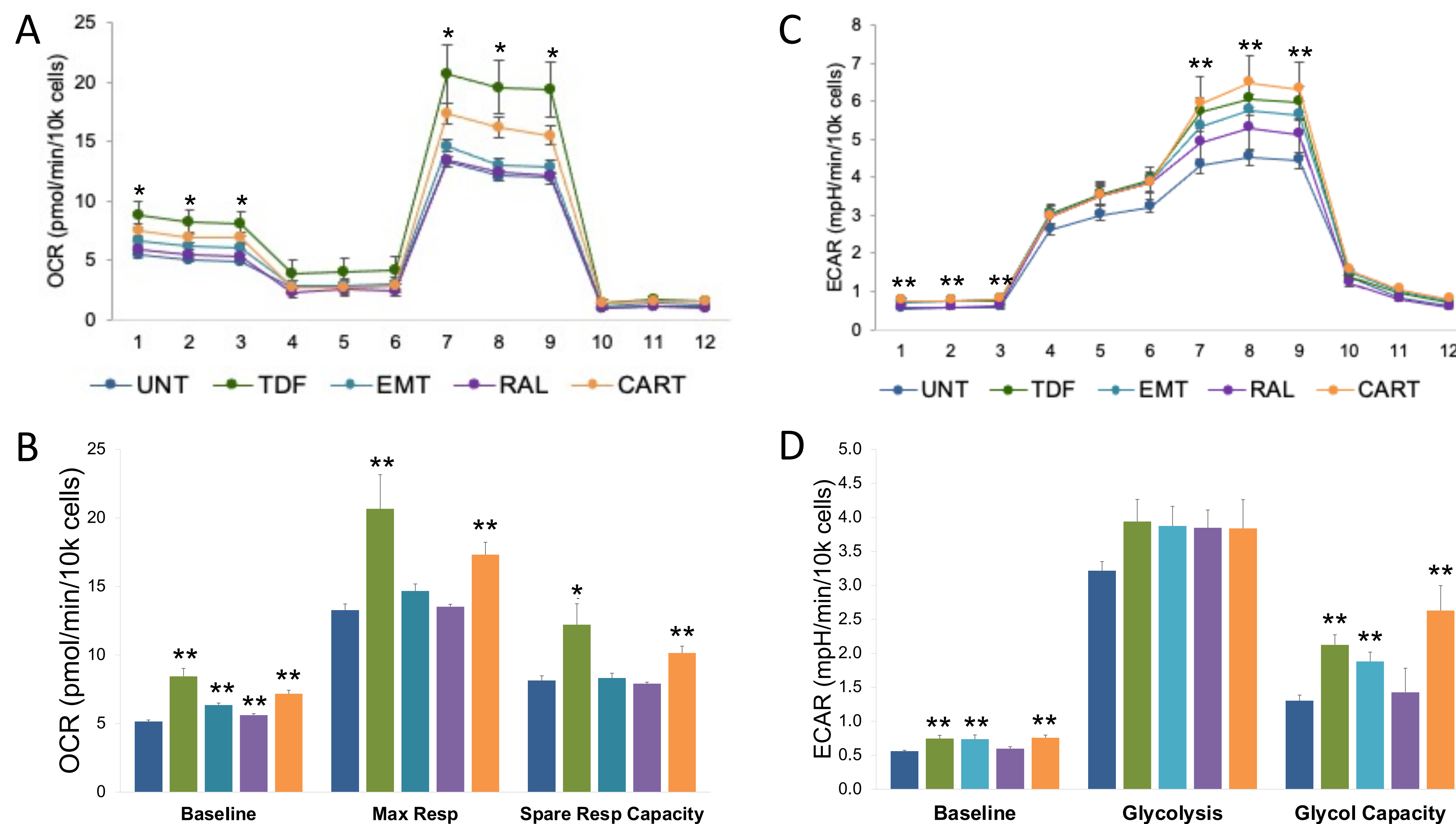


Figure 1. **A)** Metabolic profile of THP1 cells. Real-time Oxygen Consumption Rate (OCR) measured with seahorse bioanalyzer. **B)** Bar graph depicting calculated baseline respiration, maximal respiration, and spare respiratory capacity (maximal - baseline). The TDF and cART treatments are notable for their significant increase in all three metrics relative to control cells. **C)** Metabolic profile of THP1 cells under glycolytic stress test. **D)** Bar graph depicting baseline glycolysis, maximum glycolysis, and glycolytic capacity. Again, TDF and cART treatments are notable for their increase in both baseline glycolysis and glycolytic capacity relative to controls. OCR and ECAR values normalized to the number of cells. *indicates p≤0.05, ** p≤0.01 (antiretroviral treatment vs untreated controls).

Figure 3. Antiretroviral Treatment Downregulates expression of IKAROS

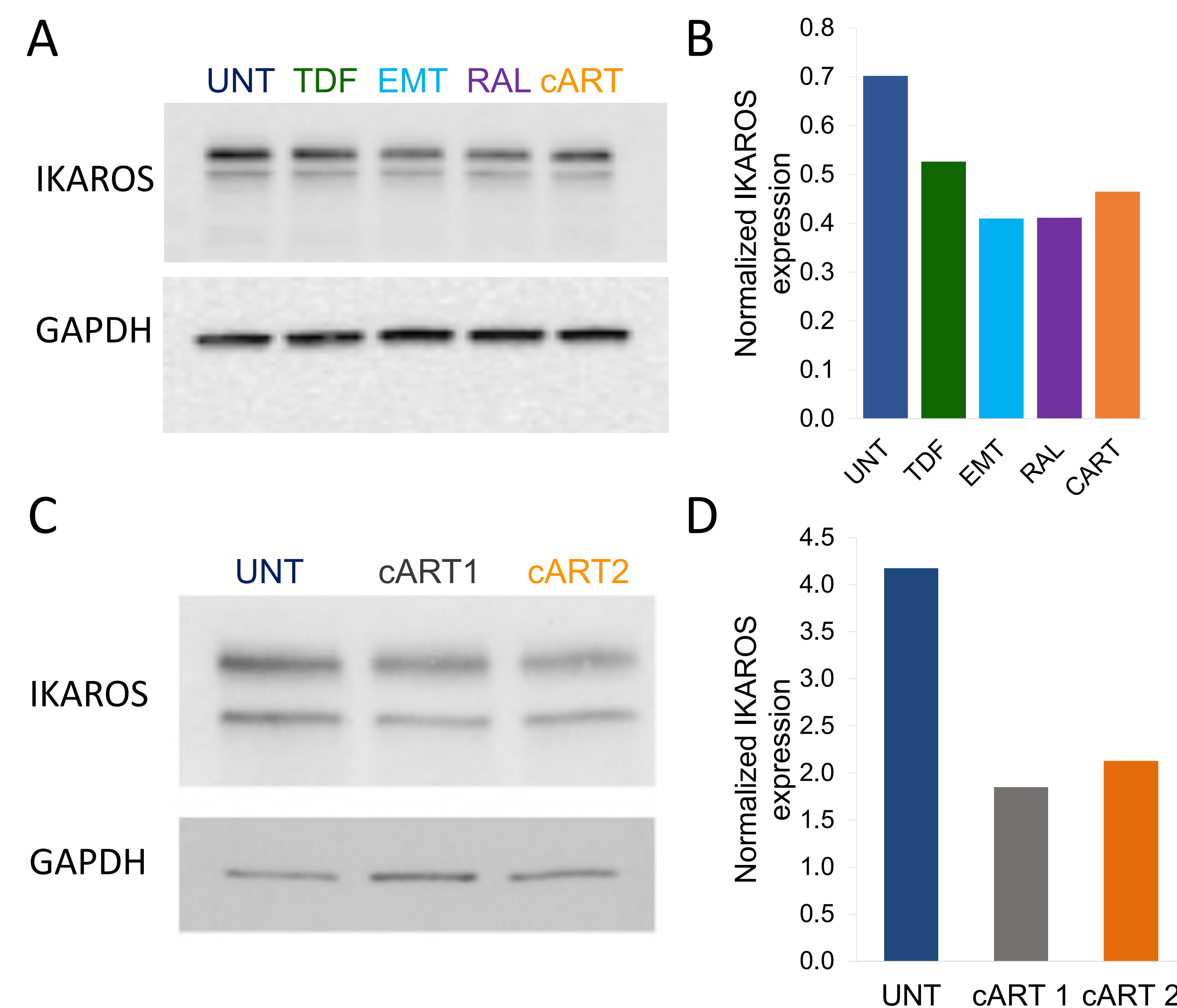


Figure 3. **A)** Western blots to detect IKAROS and GAPDH in THP1 cells treated with TDF, EMT, RAL, and cART. **B)** Quantification of the bands in Fig. 3A normalized to GAPDH. THP1 cells treated with TDF, EMT, RAL, and cART showed reduced expression of IKAROS. **C)** Western blots to detect IKAROS and GAPDH in MDMs obtained from HIV (-) individuals. **D)** Normalized to GAPDH, MDMs treated with cART1 or cART2 experienced an approximate two-fold decrease in IKAROS expression.

Conclusions

Taken together, these data indicate cART induces metabolic changes in both THP1 cells and MDMs from HIV (-) individuals that parallels with reduced levels of IKAROS expression. Specifically, the attenuation of IKAROS expression induced by cART and TDF treatment correlates with an increase in cellular oxidative phosphorylation and glycolysis in THP1 cells and oxidative phosphorylation in MDMs. This pattern matches that observed in PLWH derived MDMs. Further research is needed to determine the role of cART in the metabolic reprogramming of PLWH-MDMs, the mechanisms by which IKAROS influences metabolic pathways, and the mechanism by which cART treatment disrupts IKAROS function. Such research would provide insights into the dysfunctional immune responses of PLWH receiving cART and, perhaps, reveal treatments which avoid or address the comorbidities currently faced by patients with well-managed HIV. Given our results, THP1 cells might prove useful in such research. However, the limitations of this model must be considered with respect to PLWH derived MDMs.